Mucin 1 expression is regulated by hsa_circ_0055054/microRNA-122-5p and promotes hepatocellular carcinoma development

PENGFEI HAO[1], QI LI[2] and HAOLIANG ZHAO[1]

[1]Department of General Surgery, Third Hospital of Shanxi Medical University, Shanxi Bethune Hospital, Shanxi Academy of Medical Sciences, Tongji Shanxi Hospital, Taiyuan, Shanxi 030032, P.R. China; [2]Department of General Surgery, Shanxi Provincial People's Hospital, Taiyuan, Shanxi 030001, P.R. China

Received February 22, 2024; Accepted May 29, 2024

DOI: 10.3892/ol.2024.14537

Abstract. The abnormal expression of mucin 1 (MUC1) is a major cause of poor prognosis in patients with hepatocellular carcinoma (HCC). Competitive endogenous RNA demonstrates a novel regulatory mechanism that can affect the biological behavior of tumors. In the present study, the regulatory functions of hsa_circ_0055054 as well as those of microRNA (miR/miRNA) 122-5p on MUC1 expression and its role in HCC cell proliferation, migration and invasion, were evaluated. MUC1 expression was assessed using western blotting and reverse transcription-quantitative PCR. The phenotypic functions of the HCC cell lines were evaluated following MUC1 knockdown using Cell Counting Kit-8, wound healing and Transwell assays. Bioinformatics tools were used to identify specific miRNAs and circular (circ) RNAs that interact with and can regulate MUC1. The stability of circRNAs was assessed using a Ribonuclease R assay. The binding of circRNA/miRNA/MUC1 was assessed using dual-luciferase reporter assays and cellular function tests. Finally, *in vivo* experiments were performed using animal models. The results demonstrated that in MHCC97L cells, MUC1 and hsa_circ_0055054 were expressed at high levels while miR-122-5p was downregulated. The proliferation, migration and invasion of MHCC97L cells were suppressed by low MUC1 expression. hsa_circ_0055054 knockdown or miR-122-5p overexpression both led to a decrease in MUC1 expression. In MHCC97L cells with a low MUC1 expression caused by hsa_circ_0055054 knockdown, miR-122-5p inhibition resulted in the increased proliferation, migration and invasion of MHCC97L cells. In combination, the results of the present study indicate that hsa_circ_0055054 knockdown in MHCC97L cells leads to an increased expression of miR-122-5p and decreased expression of MUC1, which results in the inhibition of MHCC97L cell proliferation, migration and invasion.

Correspondence to: Professor Haoliang Zhao, Department of General Surgery, Third Hospital of Shanxi Medical University, Shanxi Bethune Hospital, Shanxi Academy of Medical Sciences, Tongji Shanxi Hospital, 99 Longcheng Street, Taiyuan, Shanxi 030032, P.R. China
E-mail: haoliangzhao@hotmail.com

Key words: hepatocellular carcinoma, mucin 1, hsa_circ_0055054, microRNA-122-5p, competing endogenous RNA

Introduction

Primary hepatocellular carcinoma (HCC) is currently the most common malignancy and the leading cause of cancer-related mortality worldwide. According to the International Agency for Research on Cancer, liver cancer became the 6th most prevalent disease (4.7%) and 3rd most common cause of cancer deaths (8.3%) globally in 2020 (1). However, certain drugs for HCC may not be fully effective due to the unique immune microenvironment of the liver (2-4). Therefore, further research is urgently needed to identify new targets for the treatment of HCC.

The mucin (MUC) family is a group of highly glycosylated macromolecules that are expressed at high levels in mammalian epithelial cells. They contribute to the formation of mucus barriers that prevent infection (5). Notably, certain MUCs are abnormally expressed in cancer cells and involved in tumor development, including cell proliferation, apoptosis suppression, chemical resistance, metabolic reprogramming and immune evasion (6-8). MUC1, also known as tumor-associated epithelial membrane antigen or CD227, was the first MUC to be discovered (9). MUC1 expression is primarily detected in malignant tumors that originate from epithelial cells and is characterized by increased expression with loss of polarity and structural changes (10). MUC1 can promote the evasion of stress-induced apoptosis by cancer cells by binding directly to the p53 regulatory domain and p53 response elements (11). Meanwhile, MUC1 can downregulate the expression of E-calcium mucus protein (E-cadherin), which is one of the manifestations of increased tumor cell invasion (12). According to a study of primary liver cancer, patients with a high MUC1 expression accounted for ≤68% of all patients, with the highest rate of recurrence after surgery and a positive association

with MUC1 expression intensity (13). Multiple studies have reported that the increased expression of MUC1 in HCC tissue is associated with HCC development (14-16). Therefore, down-regulating MUC1 expression in HCC may have potential in the clinical treatment of HCC. Furthermore, it is crucial to have a comprehensive understanding of the regulatory mechanism of MUC1 for the development of molecularly targeted therapies against HCC.

Circular (circ)RNAs have a loop structure, unlike traditional linear RNAs. This unique structure makes them resistant to RNA exonucleases, which increases their expression stability and decreases their susceptibility to degradation (17). circRNAs contain numerous micro (mi)RNA (miR)-binding sites that can act as 'sponges' of miRNA in cells, interfering with the expression of miRNA-regulated target genes (18). This ability of circRNAs is known as the competitive endogenous RNA mechanism (19,20). circRNAs serve a crucial regulatory role in disease development by interacting with disease-associated miRNAs. In the present study, circRNAs and miRNAs that may regulate MUC1 expression were assessed, providing new insights for the future clinical treatment of HCC.

Materials and methods

Patients and tissues. A total of five HCC tissues and their corresponding adjacent normal tissues were collected from patients who underwent surgery between March and May 2023 at the Department of General Surgery, Third Hospital of Shanxi Medical University, Shanxi Bethune Hospital (Taiyuan, China). The tissue samples were promptly preserved at -80˚C. The current study was approved by the Ethics Committee of the Third Hospital of Shanxi Medical University, Shanxi Bethune Hospital (approval no. YXLL-2023-226). All participants provided written informed consent to participate in the study.

Experimental cell lines. The human MIHA normal liver cell line and the MHCC97L, MHCC97H, Huh7, Hep3B and HCCLM3 liver cancer cell lines were purchased from Hunan Fenghui Biotechnology Co., Ltd. All cell lines were subjected to mycoplasma testing. The cells were cultured in DMEM (Boster Biological Technology) supplemented with 15% FBS (Gibco; Thermo Fisher Scientific, Inc.) and 1% penicillin/streptomycin (Boster Biological Technology). The cells were maintained at 37˚C and 5% CO_2.

Bioinformatics analysis. The best cut-off point of MUC1 expression value in all samples of HCC was taken as a threshold, and the samples were divided into MUC1 high and low expression groups. The difference in overall survival (OS) and progression-free survival (PFS) between the two groups was assessed using the log-rank test. Cox multifactorial regression analysis of MUC1 expression and clinical characteristics was used to assess whether MUC1 could serve as an independent HCC prognostic factor. Correlations were assessed using Pearson's correlation coefficient. The Cancer Genome Atlas (https://portal.gdc.cancer.gov) database was used to identify miRNAs that are downregulated in HCC [$\log_2$(fold change) <-1; P_{adj}<0.05] and have the ability to regulate MUC1 expression (correlation <-0.2; P<0.05). The Gene Expression Omnibus dataset GSE97332 (https://www.ncbi.nlm.nih.gov/geo/query/acc.cgi?acc=GSE97332) was used to identify circRNAs expressed at high levels [$\log_2$(fold change) >1; P_{adj}<0.05] in HCC. RNA22 version 2 (https://cm.jefferson.edu/rna22/Interactive/; P<0.05) and miRanda version 3.3a (http://www.bioinformatics.com.cn/local_miranda_miRNA_target_prediction_120; MaxScore >140; MaxEnergy <-15) were used to predict the relationships between miRNAs and circRNAs.

Total RNA extraction and reverse transcription-quantitative (RT-q) PCR. Total RNA was extracted from the MHCC97L and MIHA cells using TRIzol® reagent (Invitrogen; Thermo Fisher Scientific, Inc.) and quantified using Qubit 4 Fluorometer (Invitrogen; Thermo Fisher Scientific, Inc.). The M5 Super plus qPCR RT Kit with genomic DNA remover (cat. no. MF166-plus-01; Mei5 Biotechnology, Co., Ltd.) was used; 1 μl of 10X gDNA plus remover mix and 1 μg of RNA template, made up to 10 μl using (RNase)-free double-distilled H_2O and incubated at 42˚C for 2 min, then 4 μl 5X M5 RT Super plus Mix and as 6 μl (RNase)-free double-distilled H_2O, was added and incubated at 37˚C for 15 min and then 85˚C for 5 sec. The ribo*SCRIPT* mRNA/lncRNA qRT-PCR Starter Kit (cat. no. C11030-2; Guangzhou RiboBio Co., Ltd. was also employed; 1 μg of RNA template, 1 μl Random Primer, 1 μl Oligo $(dT)_{18}$, 2 μl 5X reverse transcription buffer and 2 μl RTase Mix, made up to 10 μl using (RNase)-free double-distilled H_2O and incubated at 42˚C for 60 min and then 70˚C for 10 min. These were used to reverse-transcribe miRNA, mRNA and circRNA into cDNA on the C1000 Touch Thermal Cycler (Bio-Rad Laboratories, Inc.). Subsequent RT-qPCR was performed using 2X M5 HiPer SYBR Premix EsTaq (Mei5 Biotechnology, Co., Ltd.) which included 2 μl cDNA, 12.5 μl 2X M5 Hiper SYBR Premix EsTaq, 0.5 μl forward and reverse primers and 9.5 μl ribonuclease (RNase)-free double-distilled H_2O added to the CFX96 Touch Real-Time PCR Detection System (Bio-Rad Laboratories). The thermocycling conditions were as follows: 95˚C for 30 sec, followed by 40 cycles of 95˚C for 5 sec and 60˚C for 30 sec. The relative expression of the target mRNA and miRNA were quantified using the $2^{-\Delta\Delta Cq}$ method (21). The primers sequences were as follows: MUC1, 5'-CTGCTGGTGCTGGTCTGTGTTC-3' forward and 5'-GGGTACTCGCTCATAGGATGGTAGG-3' reverse; GAPDH, 5'-CAGGAGGCATTGCTGATGAT-3' forward and 5'-GAAGGCTGGGGCTCATTT-3' reverse; U6, 5'-CTCGCTTCGGCAGCACA-3' forward and 5'-AACGCTTCACGAATTTGCGT-3' reverse; miR-122-5p, 5'-CCTGGAGTGTGACAATGGTGTTTG-3' forward; hsa_circ_0055054, 5'-TGATGTTGCAGCAGTAGTGGATGG-3' forward and 5'-CCACACGAGAGAGATTGCAGC-3' reverse; linear_0055054, 5'-GCTGCAATCTCTCTCGTGTGG-3' forward and 5'-TCCATCCACTACTGCTGCAACATC-3' reverse. The aforementioned sequences were purchased from Sangon Biotech Co., Ltd. GAPDH or U6 were used as controls for mRNA, circRNA or miRNA. The reverse miR-122-5p sequence (cat. no. B661601; Sangon Biotech Co., Ltd.) could not be disclosed due to confidentiality agreements with the reagent company.

RNase R assay. To evaluate the stabilization of hsa_circ_0055054, the following reaction system was prepared

in sterile microcentrifuge tubes: 17.9 μl diethyl pyrocarbonate-treated water, 1 μg template total RNA, 2 μl 10X RNase R Reaction Buffer and 2 U RNase R (20 U/μl; Shanghai Yeasen Biotechnology Co., Ltd.). Subsequently, the mixture was incubated for 15 min at 37˚C. RT-qPCR was used to detect the relative abundance of circRNA and linear RNA.

Western blotting. Protein were extracted from MHCC97L cells and MIHA cells were using radioimmunoprecipitation assay lysis buffer (Boster Biological Technology) and 1% protease/phosphatase inhibitor cocktail (MedChemExpress). Protein concentration was determined using the bicinchoninic acid protein assay kit (Boster Biological Technology). The proteins were diluted to the desired concentration by adding 5X SDS-PAGE loading buffer (Boster Biological Technology) and PBS (Boster Biological Technology). The proteins were subsequently denatured through incubation for 5 min at 95˚C in a metal bath. The proteins (20 μg per lane for each sample) were separated by 10% SDS-PAGE and subsequently transferred onto a PVDF membrane that had been previously treated with anhydrous ethanol for 1 min. The membrane was blocked with protein-free rapid sealing solution (Boster Biological Technology) for 20 min at room temperature, after which anti-MUC1 rabbit polyclonal antibodies (1:1,500; cat. no. A0333; ABclonal Biotech Co., Ltd.) and anti-β-actin polyclonal antibodies (1:10,000; cat. no. BA2305; Boster Biological Technology) were added and incubated overnight at 4˚C. The membrane was washed for 30 min with TBS containing 0.05% Tween-20. Subsequently, secondary antibodies (HRP-conjugated AffiniPure goat anti-rabbit IgG; 1:20,000; cat. no. BA1039; Boster Biological Technology) was added, and the samples were incubated at room temperature for 2 h and washed three times for 10 min each. Eventually, protein visualization was performed using the ChemiDoc Imaging System (Bio-Rad Laboratories, Inc.) and the FG supersensitive ECL luminescence reagent (Dalian Meilum Biotechnology Co., Ltd.).

Cell transfection. The following specific small interfering (si)RNA sequences were purchased from Sangon Biotech Co., Ltd.: si-MUC1, sense: 5'-CUCUCGAUAUAACCUGACGAUTT-3' and antisense: 5'-AUCGUCAGGUUAUAUCGAGAGTT-3'; si-negative control (NC), sense: 5'-UUCUCCGAACGUGUCACGUTT-3' and antisense: 5'-ACGUGACACGUUCGGAGAATT-3'; miR-122-5p mimic, sense: 5'-UGGAGUGUGACAAUGGUGUUUG-3' and antisense: 5'-AACACCAUUGUCACACUCCAUU-3'; miR-122-5p inhibitor, sense: 5'-CAAACACCAUUGUCACACUCCA-3'; miR-122-5p mimic-NC, sense: 5'-UUGUACUACACAAAAGUACUG-3' and antisense: 5'-GUACUUUUGUGUAGUACAAUU-3'; miR-122-5p inhibitor-NC, sense: 5'-CAGUACUUUUGUGUAGUACAA-3'; and si-hsa_circ_0055054, sense: 5'-GCGUCAUCUUUGCAAAGACAATT-3' and antisense: 5'-UUGUCUUUGCAAAGAUGACGCTT-3'. For si-MUC1 and si-hsa_circ_0055054, a universal negative control was used, namely a common negative control with no homology to the target gene sequence and no significant homology to other mRNAs of the same species. MHCC97L cells were cultured in 24-well plates (3x10^5 cells/well) or 96-well plates (2x10^4 cells/well) and incubated for 24 h. Subsequently, 1.25 μl 20 μM miRNA was diluted with 30 μl 1X ribo*FECT*™ CP buffer (Guangzhou RiboBio Co., Ltd.). A total of 3 μl riboFECT CP reagent was then added, the solution was mixed gently and incubated at room temperature for 15 min, followed by incubation with DMEM supplemented with 15% FBS at 37˚C and 5% CO_2 for 48 h. After 48 h, RNAs and proteins were extracted as in the western blotting and RT-qPCR section from the cells and subsequently validated by western blotting and RT-qPCR.

Dual-luciferase reporter assay. The sequences containing miR-122-5p-binding sites in hsa_circ_0055054 and MUC1 3'-UTR, as well as site-directed mutation of the binding sites produced by Sangon Biotech Co., Ltd. (sequences as in Cell transfection section), were subcloned into pmirGLO reporting luciferase vectors (Promega Corporation). The wild-type (WT) or mutant (MT) luciferase reporter vectors were constructed. Subsequently, miR-122-5p mimic or miR-122-5p mimic-NC vectors were co-transfected into MHCC97L cells with the reporter plasmids by Lipofectamine® 2000 (Invitrogen; Thermo Fisher Scientific, Inc.). After 48 h, luciferase activity was measured using the Dual-Luciferase Reporter Assay System (Promega Corporation)and expressed as relative activity. In the two groups transfected with the same Luciferase plasmid, the relative expression of luciferase in the miRNA-NC group was normalized to 1, and the value of the target miRNA group was divided by the value of the miRNA-NC group to obtain the value of its relative expression of luciferase.

Cell proliferation assay. MHCC97L cells in the logarithmic growth phase with a cell fusion rate of ~85% were made into a cell suspension at a concentration of 1x10^5 cells/ml. Subsequently, 100 μl cell suspension was added to each well in a 96-well plate. Following overnight incubation at 37˚C and 5% CO_2, the cells were transfected as aforementioned. Cell proliferation was assessed using the Cell Counting Kit-8 (Boster Biological Technology). The plate was incubated for 1 h in a cell incubator. Subsequently, optical density values were assessed using a microplate reader (Thermo Fisher Scientific, Inc.) at 450 nm.

Wound healing assay. The MHCC97L cells were cultured in a 24-well plate at a density of 2x10^5 cells/well. When the cell fusion rate reached 100% confluence, the culture medium was removed and wounds were made by a 200 μl pipette tip. Then serum-free medium was added. Cellular wound healing was observed under an inverted light microscope (magnification, x100; Nikon Corporation) at both the 0 and 48 h timepoints at the same location. The experiment was repeated three times, and the relative scratch width was used to quantify the migratory ability of the HCC cells. The relative scratch width was calculated by dividing the distance of the scratch zone at 48 h by the distance of the scratch zone at 0 h, subtracting this result from 1, and then multiplying it by 100%.

Cell invasion assays. Experiments were performed using transfected MHCC97L cells in a Transwell chamber containing 60 μl Matrigel (BD Biosciences) diluted at 1:8 with serum-free medium (Boster Biological Technology) and incubated 2 h at 37˚C and 5% CO_2. Then the excess liquid

of the upper chamber in the completed incubation chambers was aspirated and 100 μl of serum-free medium was added to each well and incubated for 30 min at 37˚C and 5% CO_2. The upper compartment of the 24-well Transwell chamber (8-mm pore size; Guangzhou Jet Bio-Filtration Co., Ltd.) contained $3x10^5$ cells and 200 μl DMEM (without serum), whilst the lower compartment contained 600 μl complete medium (20% FBS). After 24 h of continuous incubation at 37˚C and 5% CO_2, the cells in the lower layer were fixed with 4% paraformaldehyde for 20 min and stained with 0.1% crystal violet for 10 min at room temperature. Subsequently, the cells were observed under an inverted light microscope (magnification, x100; Nikon Corporation).

In vivo study. Subcutaneous transplantation models of tumors were constructed using 4-week-old female BALB/c nude mice provided by SPF Biotechnology Co, Ltd. To construct short hairpin (sh)RNA, si-NC and si-hsa_circ_0055054 were selected and assessed in cellular experiments and lentivirally packaged. These cells were then turned into stable transfected MHCC97L cells by Suzhou Haixing biotechnology Co., Ltd. The mice were acclimatized to the specific pathogen-free animal laboratory for 1 week under a 12-h light/dark cycle. Following acclimatization, 10 mice were randomly assigned to two groups of five mice using a random number table. Stably transfected MHCC97L cells harboring sh-NC or sh-hsa_circ_0055054 were thawed and the expression levels of hsa_circ_0055054 were determined by RT-qPCR as aforementioned. A total of ~$5x10^6$ MHCC97L cells (100 μl) transfected with sh-NC or sh-hsa_circ_0055054 were subcutaneously injected into the mid-posterior area of the right axilla of both groups of mice. The mice were provided unrestricted access to food and water at a temperature of 25˚C throughout the experimentation period. The mice with tumors were examined three times a week, and the maximum allowable tumor volume (length x $width^2$ x 0.5) was 2 cm^3. In addition, if the nude mice lost >20% of their body weight, showed obvious pain or self-injury, developed ulcers or infections at the site of subcutaneous tumors, or the tumors metastasized to other parts of the body during the course of the experiments, the experiments were terminated, and the animals were euthanized. After 4 weeks, the mice were euthanized by CO_2 overdose: CO_2 was infused into the euthanasia chamber at a rate of 30% of its volume per min, and the tumors were removed. Subsequently, the volume and weight of each tumor was calculated, and the tumors were fixed with 4% paraformaldehyde (Boster Biological Technology) for further experiments. During euthanasia, if an animal had no respiration or pulse, no heartbeat for >5 min determined by stethoscope or by touching the heart in the chest cavity, and if the corneal reflexes of the animal were absent, pupils were dilated, and neural reflexes had disappeared, the animal was considered to be dead. The animal experimental procedures were approved and performed following the guidelines of the Animal Ethics Committee of Shanxi Provincial People's Hospital (approval no. 2023-451).

Statistical analysis. Data are expressed as the mean ± standard deviation, and all experiments were repeated three times. SPSS (version 26.0; IBM Corp.) was used for statistical analysis. The graphs were produced using GraphPad Prism (version 9.5.1; Dotmatics) and ImageJ (version 1.5.4, National Institutes of Health). Data from proliferation, migration, invasion, tumor volume and weight, western blotting and RT-qPCR were analyzed according to the type of data and methods of comparison, depending on whether the data conformed to a normal distribution. A paired Student's t-test was used to assess the mean values of the HCC tissues and the corresponding paraneoplastic normal tissues. The mean values between the other two groups were compared using an unpaired Student's t-test, and differences between multiple groups were compared using one-way ANOVA with Dunnett's post-hoc test. $P<0.05$ was considered to indicate a statistically significant difference.

Results

High MUC1 expression in HCC is associated with a poor survival rate. The bioinformatics data demonstrated that MUC1 was expressed at significantly higher levels in HCC tissues compared with normal tissues (Fig. 1A). Furthermore, Kaplan-Meier survival curve analysis indicated that patients with a high MUC1 expression had significantly shorter OS compared with those with a low MUC1 expression (Fig. 1B). Similarly, patients with high MUC1 expression had a significantly shorter PFS than those with low MUC1 expression (Fig. 1C). However, further data analysis revealed that MUC1 expression in HCC was not significantly associated with the clinical characteristics of the patients (Fig. 1D and E). RT-qPCR (Fig. 1F) and western blotting (Fig. 1G) demonstrated that MUC1 was expressed at significantly higher levels in HCC tissues than in normal tissues. These findings suggest that MUC1 overexpression is associated with HCC development.

MUC1 downregulation impedes the function of HCC. MUC1 expression was evaluated in the five liver cancer lines MHCC97L, MHCC97H, Huh7, Hep3B and HCCLM3 using western blotting and RT-qPCR. MIHA human normal liver cells were used as a control. The results revealed that the levels of MUC1 in liver cancer cells, particularly in MHCC97L cells, were significantly higher than those in control cells (Fig. 2A). Therefore, the MHCC97L cell line was selected for subsequent experiments. The experimental group was co-cultured with si-MUC1, whilst the control group received either only the transfection reagent or the transfection reagent and si-NC. The successful transfection of si-MUC1 and a notable reduction in MUC1 expression were confirmed by both western blotting (Fig. 2B) and RT-qPCR (Fig. 2C). Furthermore, reducing the expression of MUC1 in MHCC97L cells led to a significant reduction in migration (Fig. 2D), invasion (Fig. 2E) and proliferation (Fig. 2F) compared with the Blank group.

MUC1 is regulated by miR-122-5p. A total of 39 downregulated miRNAs were identified in HCC, five of which were significantly negatively associated with MUC1 expression. Considering its expression level and negative associated with MUC1, miR-122-5p was selected for further experiments (Fig. 3A). Pearson's correlation coefficient and RT-qPCR revealed a significant negative correlation between MUC1 and miR-122-5p (Fig. 3B-D) and the binding regions between

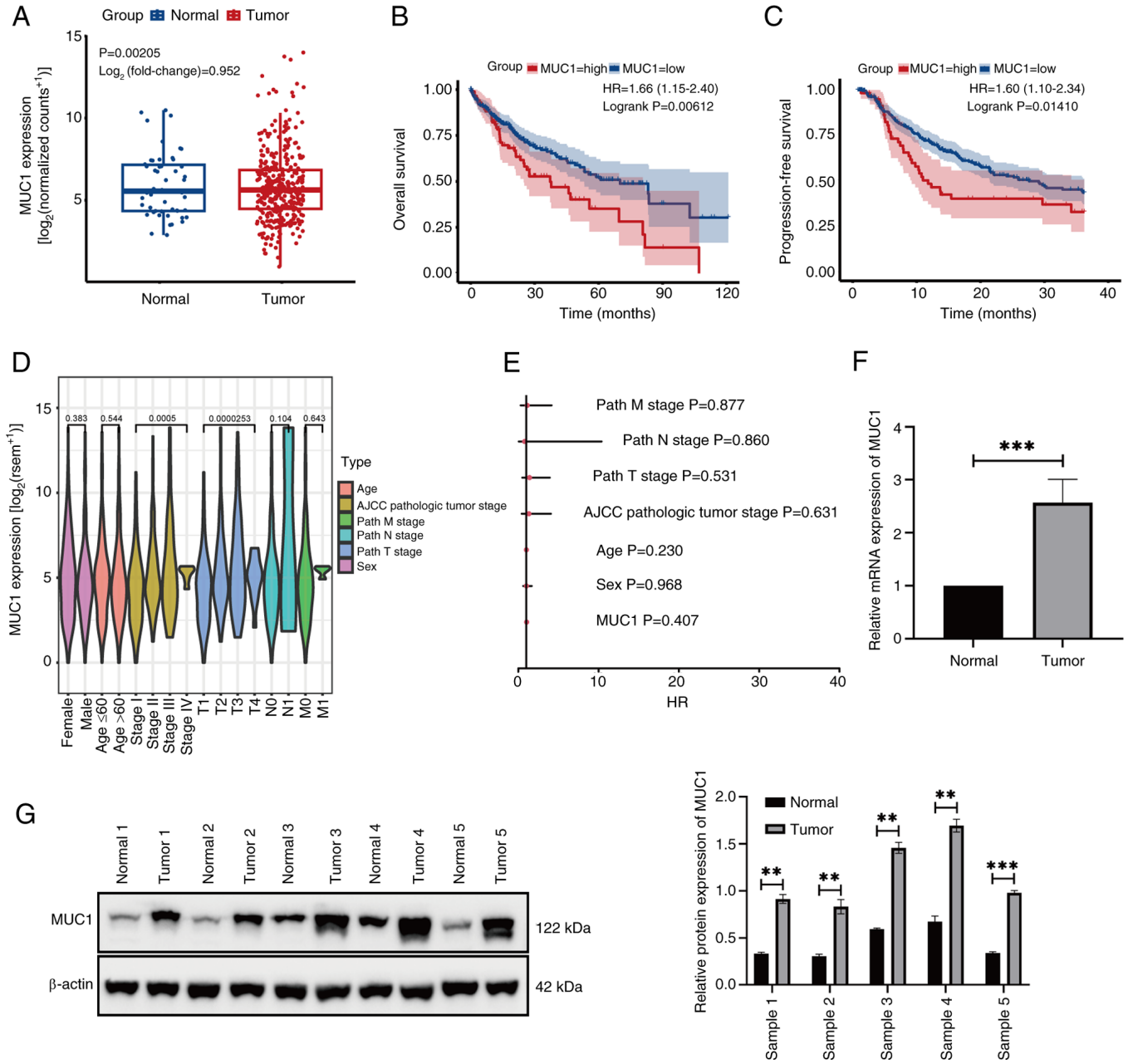

Figure 1. Expression of MUC1 in HCC tissues. (A) MUC1 expression in HCC tissues and corresponding adjacent normal tissues using data from the The Cancer Genome Atlas database. (B) Overall and (C) progression-free survival in the high and low MUC1 expression groups. (D) Association between MUC1 expression in HCC and the clinical characteristics of patients. (E) Cox's multifactorial regression analysis of MUC1 expression in HCC and the clinical characteristics of patients. (F) Reverse transcription-quantitative PCR and (G) western blotting assessment of MUC1 expression in HCC tissues compared with the corresponding adjacent normal tissues in five samples. **P<0.01 and ***P<0.001. MUC1, mucin 1; HCC, hepatocellular carcinoma; HR, hazard ratio; AJCC, American Joint Committee on Cancer; T, tumor; N, node; M, metastasis.

MUC1 and miR-122-5p were identified (Fig. 3E). In MHCC97L cells, the co-culture of the miR-122-5p mimic with WT-MUC1 resulted in a significant decrease in dual-luciferase reporter activity, whilst no significant change was observed when the cells were co-transfected with MT-MUC1 (Fig. 3F). These findings suggest that miR-122-5p can bind to MUC1.

Effects of miR-122-5p on MHCC97L cells through the regulation of MUC1 expression. To assess the role of miR-122-5p in HCC, MHCC97L cells were transfected with miR-122-5p mimic or miR-122-5p inhibitor. RT-qPCR and western blotting were used to determine the expression of the miR-122-5p mimic/inhibitor and MUC1 in the transfected cells. The results demonstrated that miR-122-5p mimic was successfully transfected into MHCC97L cells (Fig. 4A). A significant reduction in MUC1 expression was observed in MHCC97L cells transfected with the miR-122-5p mimic compared with the Blank group (Fig. 4B). Subsequently, miR-122-5p inhibitor was used to evaluate the results of the previous experiments by transfecting MHCC97L cells. The results revealed that miR-122-5p inhibitor was successfully transfected into MHCC97L cells (Fig. 4C) and MUC1 expression was significantly elevated in the experimental group compared with the Blank group (Fig. 4D). These findings were consistent with aforementioned

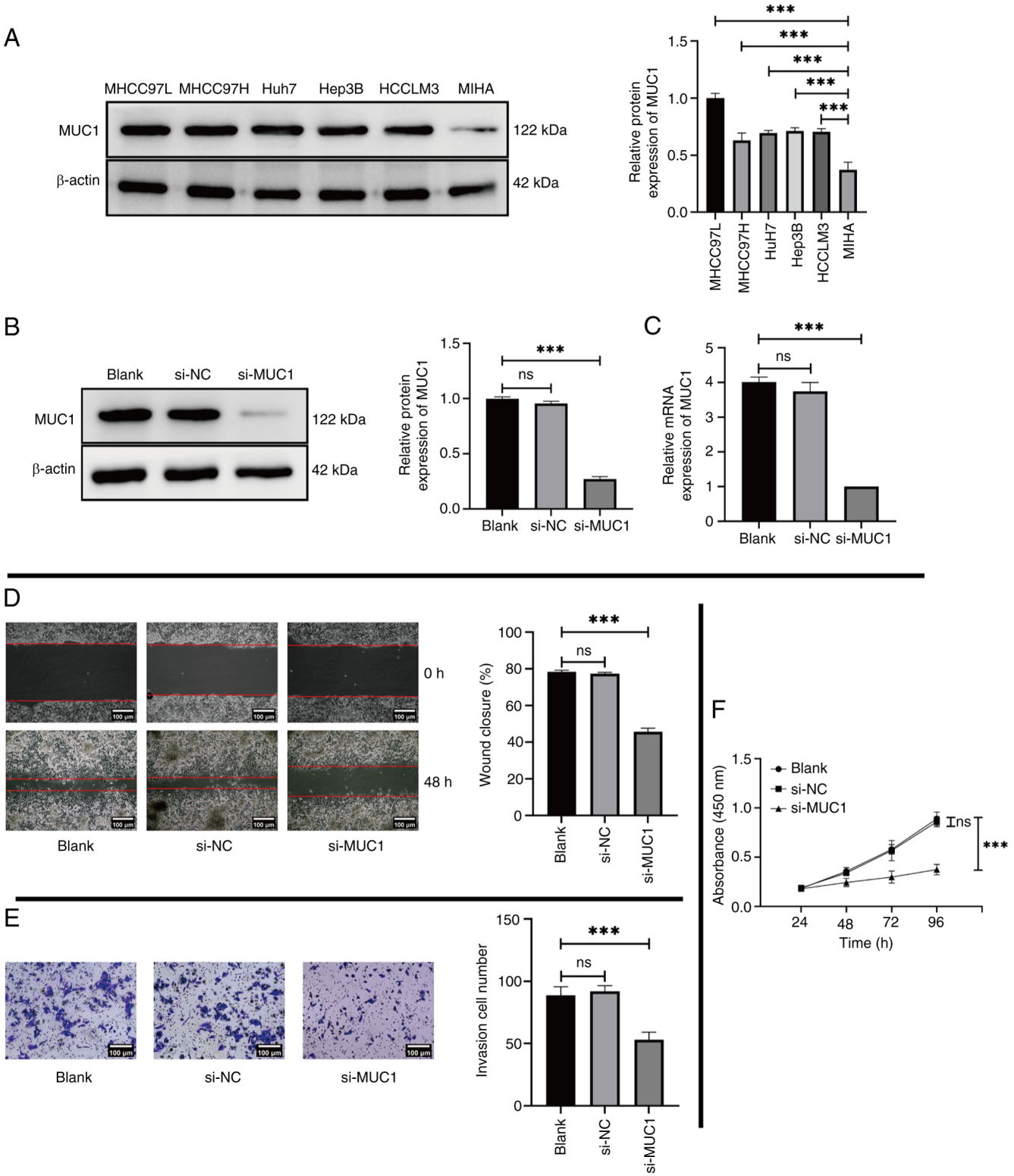

Figure 2. Expression of MUC1 in several HCC cell lines and the impact of MUC1 knockdown on the phenotypic function of HCC cells. (A) Expression level of MUC1 in MHCC97L, MHCC97H, Huh7, Hep3B and HCCLM3 cells was assessed using western blotting, with MIHA cells used as control. MUC1 expression in MHCC97L cells following transfection with only transfection reagents (Blank) compared with si-NC and si-MUC1, assessed using (B) western blotting and (C) reverse transcription-quantitative PCR. (D) MHCC97L cell migration evaluated using a wound healing assay following transfection with only transfection reagents (Blank) and compared with si-NC and si-MUC1 (scale bar, 100 μm). (E) Cell invasion assay assessing the invasion of MHCC97L cells in the Blank group compared with si-NC and si-MUC1 groups (scale bar, 100 μm). (F) MHCC97L cell proliferation following transfection with only transfection reagents (Blank) compared with si-NC and si-MUC1 was assessed using the Cell Counting Kit-8 assay. ***P<0.001. ns, not significant; MUC1, mucin 1; HCC, hepatocellular carcinoma; si, small interfering; NC, negative control.

bioinformatics analysis, which demonstrate that miR-122-5p negatively regulates MUC1 expression. At the cellular level, MHCC97L cells transfected with the miR-122-5p mimic were used to perform cell phenotype experiments. The results

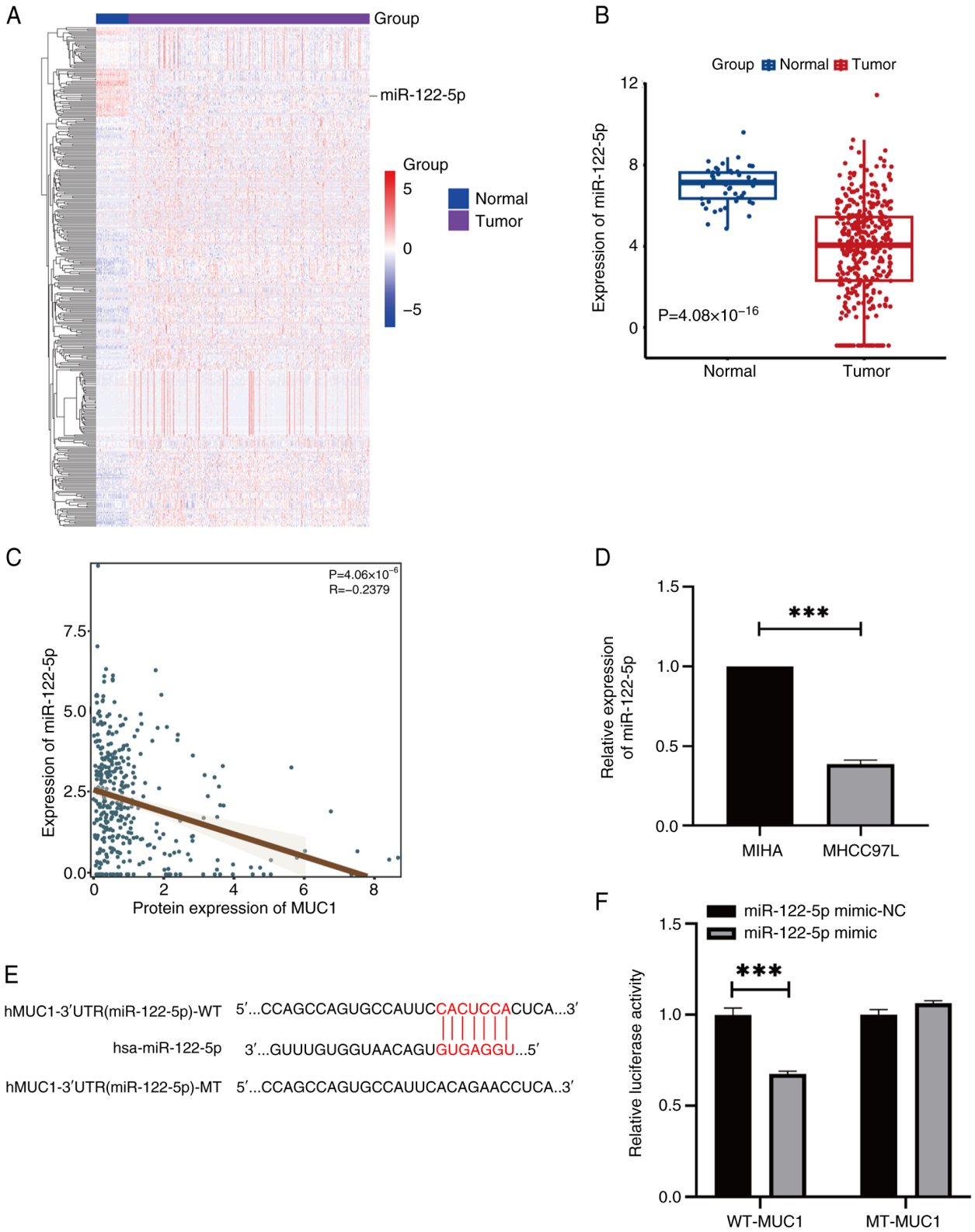

Figure 3. MUC1 expression is regulated by miR-122-5p. (A) Screening for differential miRNAs in HCC tissues by TCGA database. (B) Levels of miR-122-5p in both HCC and the corresponding adjacent normal tissues were assessed through TCGA database. (C) Correlation between MUC1 and miR-122-5p expression. (D) Expression of miR-122-5p in MHCC97L cells compared with MIHA cells, assessed using reverse transcription-quantitative PCR. (E) Complementary regions of MUC1 and miR-122-5p. (F) Dual-luciferase reporter assay demonstrated that miR-122-5p targeted MUC1. ***P<0.001. MUC1, mucin 1; miRNA/miR, microRNA; TCGA, The Cancer Genome Atlas; HCC, hepatocellular carcinoma; WT, wild-type; MT, mutant; NC, negative control.

revealed significant decreases in the migration (Fig. 4E), invasion (Fig. 4F) and proliferation (Fig. 4G) of the miR-122-5p mimic group compared with the Blank group.

hsa_circ_0055054 can bind to miR-122-5p. By analyzing the dataset GSE97332, it was found that 415 circRNAs were specifically expressed at high levels in HCC. RNA22 and miRanda

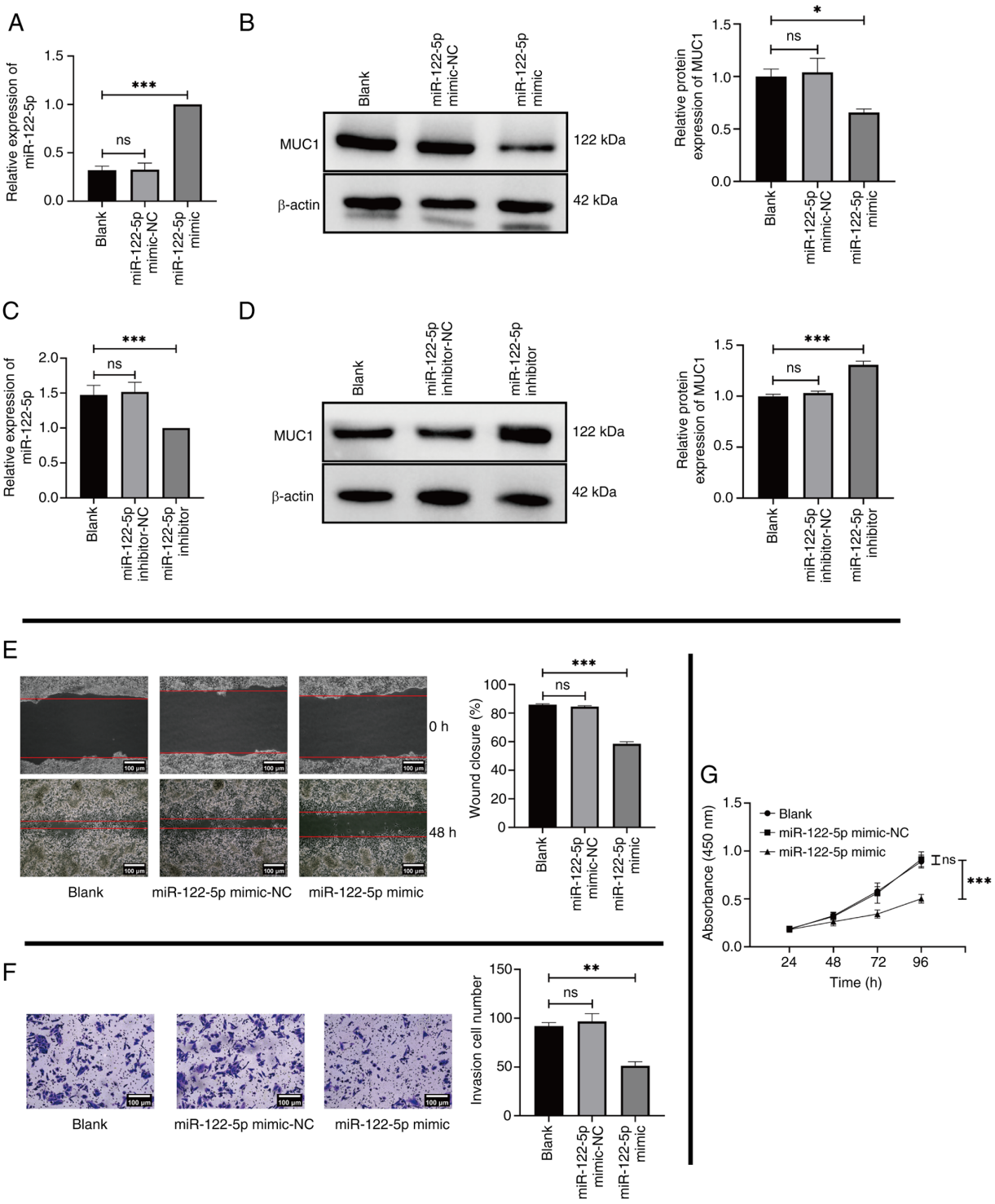

Figure 4. Regulation of MUC1 expression by miR-122-5p affects MHCC97L cells. (A) RT-qPCR for the detection of miR-122-5p expression and (B) western blotting for the detection of MUC1 expression in MHCC97L cells following transfection with only transfection reagents (Blank) compared with miR-122-5p mimic-NC and miR-122-5p mimic. (C) RT-qPCR for the detection of miR-122-5p expression and (D) western blotting for the detection of MUC1 expression in MHCC97L cells following transfection with only transfection reagents (Blank) compared with miR-122-5p inhibitor-NC and miR-122-5p inhibitor. (E) MHCC97L cell migration evaluated using a wound healing assay following transfection with only transfection reagents (Blank) compared with miR-122-5p mimic-NC and miR-122-5p mimic (scale bar, 100 μm). (F) Cell invasion assay performed to assess the invasion of MHCC97L cells in the Blank group compared with miR-122-5p mimic-NC and miR-122-5p mimic group (scale bar, 100 μm). (G) MHCC97L cell proliferation following transfection with only transfection reagents (Blank) compared with miR-122-5p mimic-NC and miR-122-5p mimic, assessed using the Cell Counting Kit-8 assay. *P<0.05; **P<0.01; ***P<0.001. ns, not significant; MUC1, mucin 1; miR, microRNA; RT-qPCR, reverse transcription-quantitative PCR; NC, negative control.

were then used to predict the binding sites of these circRNAs to miR-122-5p. It was determined that hsa_circ_0055054 satisfied the study criteria (Fig. 5A and B) and contained a binding site for miR-122-5p (Fig. 5C). Subsequently, RT-qPCR revealed that hsa_circ_0055054 was significantly expressed at high levels in MHCC97L cells compared with in MIHA

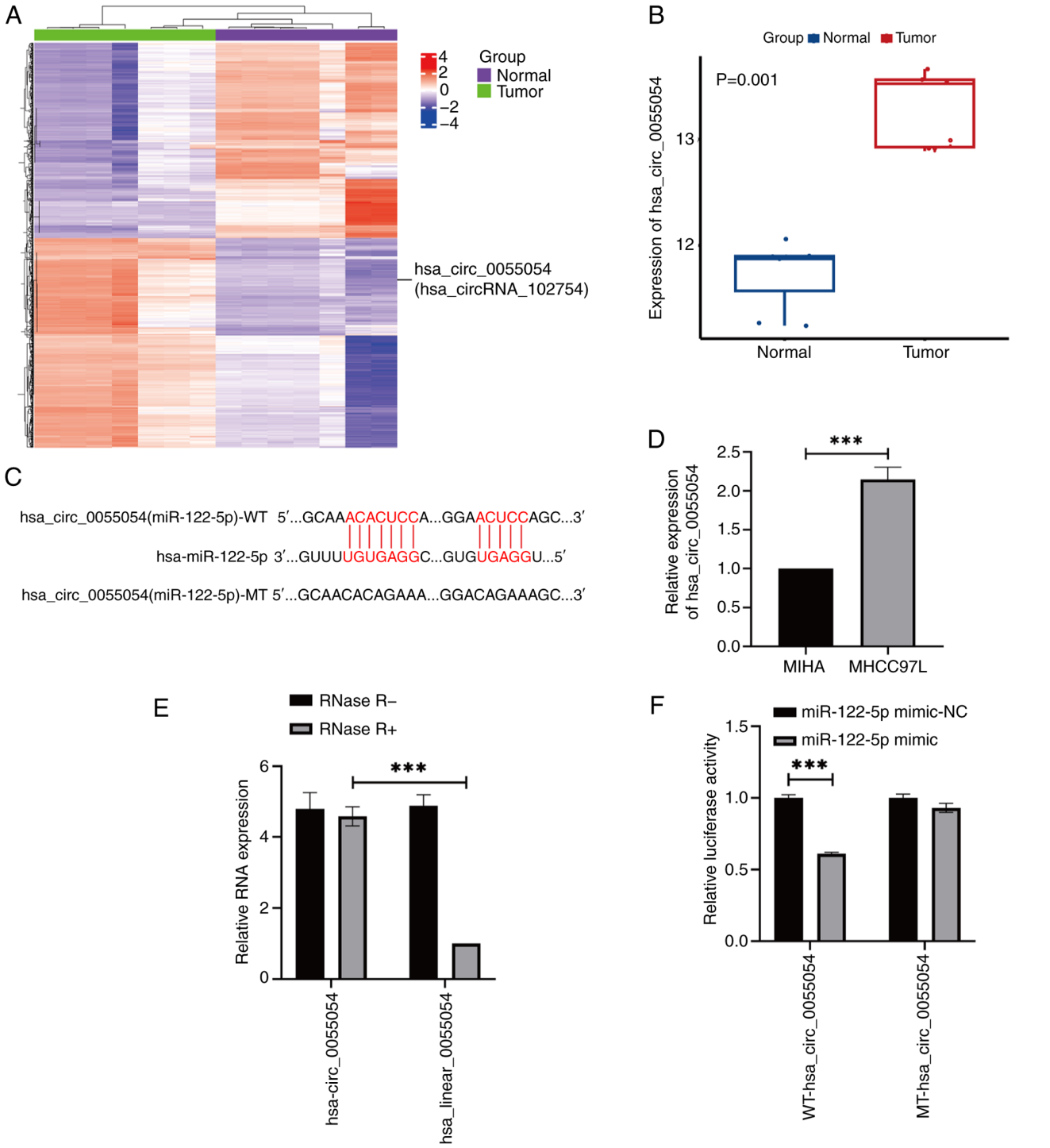

Figure 5. hsa_circ_0055054 can bind to miR-122-5p. (A) Heatmap of differential circRNA expression profile clustering in HCC and corresponding adjacent normal tissues. (B) Comparison of hsa_circ_0055054 expression in HCC tissues and corresponding adjacent normal tissues in the GEO database. (C) Complementary regions of hsa_circ_0055054 and miR-122-5p. (D) Assessment of hsa_circ_0055054 expression in the MHCC97L cell line was compared with that in the control MIHA cell line using reverse transcription-quantitative PCR. (E) Ribonuclease R treatment assay confirmed that hsa_circ_0055054 was a circRNA. (F) Dual-luciferase reporter assay demonstrated that hsa_circ_0055054 targeted miR-122-5p. ***P<0.001. circRNA, circular RNA; HCC, hepatocellular carcinoma; miR, microRNA; WT, wild-type; MT, mutant-type; circ, circular RNA; NC, negative control.

cells (Fig. 5D). The RNase R assay was then used to ascertain the stability of hsa_circ_0055054 in MHCC97L cells. After RNase R treatment the linear RNA was almost completely digested and the circRNA was enriched. The findings indicated that hsa_circ_0055054 exhibited resistance to RNase R treatments, whereas linear_0055054 was significantly degraded (Fig. 5E). Furthermore, dual-luciferase activity in MHCC97L cells significantly decreased following transfection with the miR-122-5p mimic containing WT-hsa_circ_0055054. However, no significant change in dual-luciferase reporter activity was observed when the miR-122-5p mimic was co-transfected with MT-hsa_circ_0055054 (Fig. 5F). This finding suggests an interaction between miR-122-5p and hsa_circ_0055054.

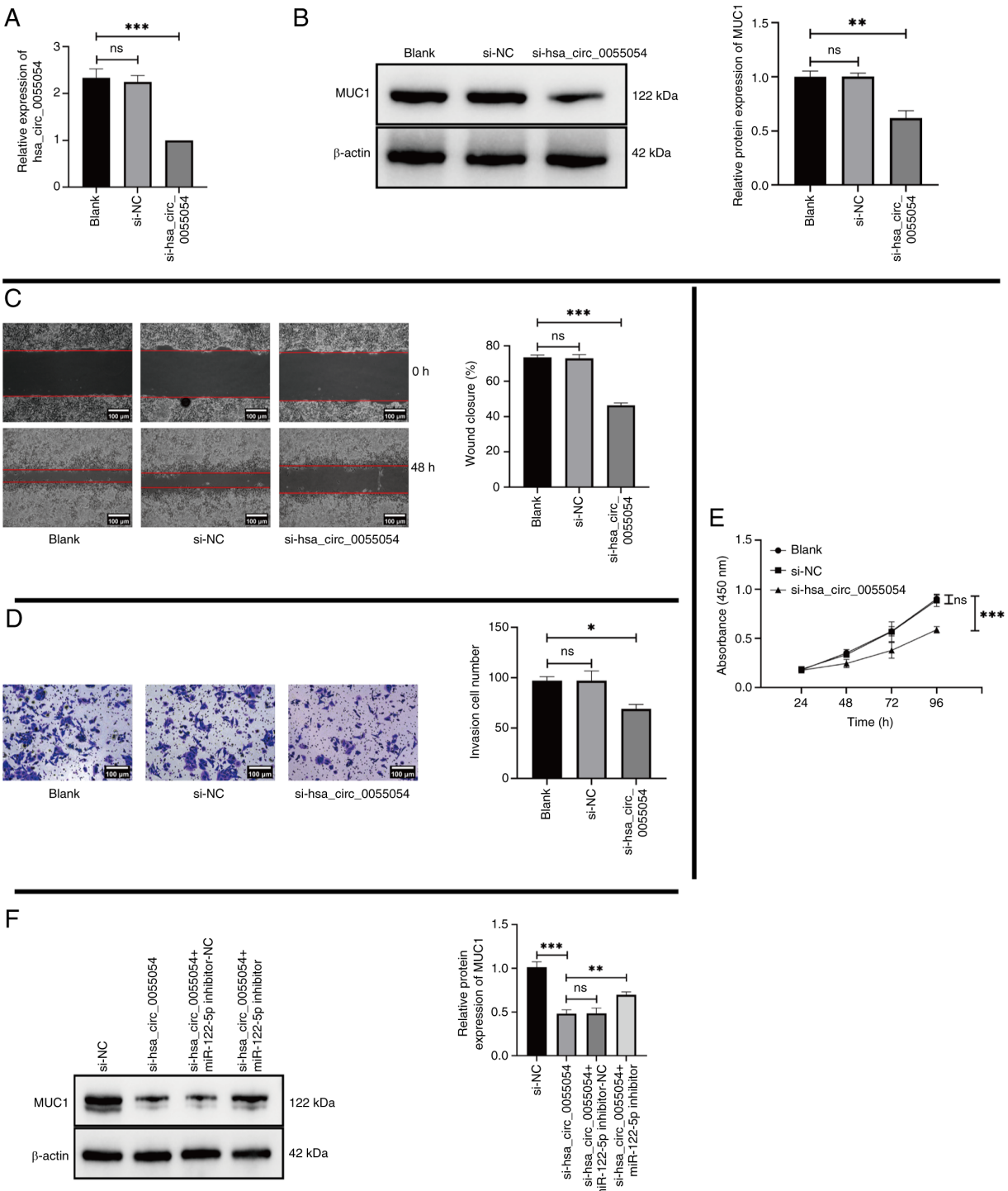

Figure 6. hsa_circ_0055054 promotes MHCC97L cell proliferation, migration and invasion by binding to miR-122-5p. (A) Reverse transcription-quantitative PCR for the detection of hsa_circ_0055054 expression and (B) western blotting for the detection of MUC1 expression in MHCC97L cells following transfection with only transfection reagents (Blank) compared with si-NC and si-hsa_circ_0055054. (C) Migration of MHCC97L cells evaluated using a wound healing assay following transfection with only transfection reagents (Blank) compared with si-NC and si-hsa_circ_0055054 (scale bar, 100 μm). (D) Cell invasion assay performed to assess the invasion of MHCC97L cells in the Blank group compared with si-NC and si-hsa_circ_0055054 groups (scale bar, 100 μm). (E) MHCC97L cell proliferation following transfection with only transfection reagents (Blank) compared with si-NC and si-hsa_circ_0055054, assessed using the Cell Counting Kit-8 assay. (F) Western blotting for the detection of MUC1 expression in MHCC97L cells following transfection with si-hsa_circ_0055054 compared with si-NC, si-hsa_circ_0055054 with miR-122-5p inhibitor-NC, and si-hsa_circ_0055054 with miR-122-5p inhibitor. *P<0.05; **P<0.01; ***P<0.001. ns, not significant; miR, microRNA; MUC1, mucin 1; si, small interfering RNA; NC, negative control; circ, circular RNA.

hsa_circ_0055054 promotes MHCC97L cell proliferation, migration and invasion by binding to miR-122-5p. To assess whether hsa_circ_0055054 regulates the expression of MUC1 and its potential regulatory effects, MHCC97L cells were co-cultured with si-NC or si-hsa_circ_0055054. RT-qPCR and western blotting revealed significantly lower expression levels of hsa_circ_0055054 (Fig. 6A) and MUC1 (Fig. 6B) in the si-hsa_circ_0055054 group compared with that in the

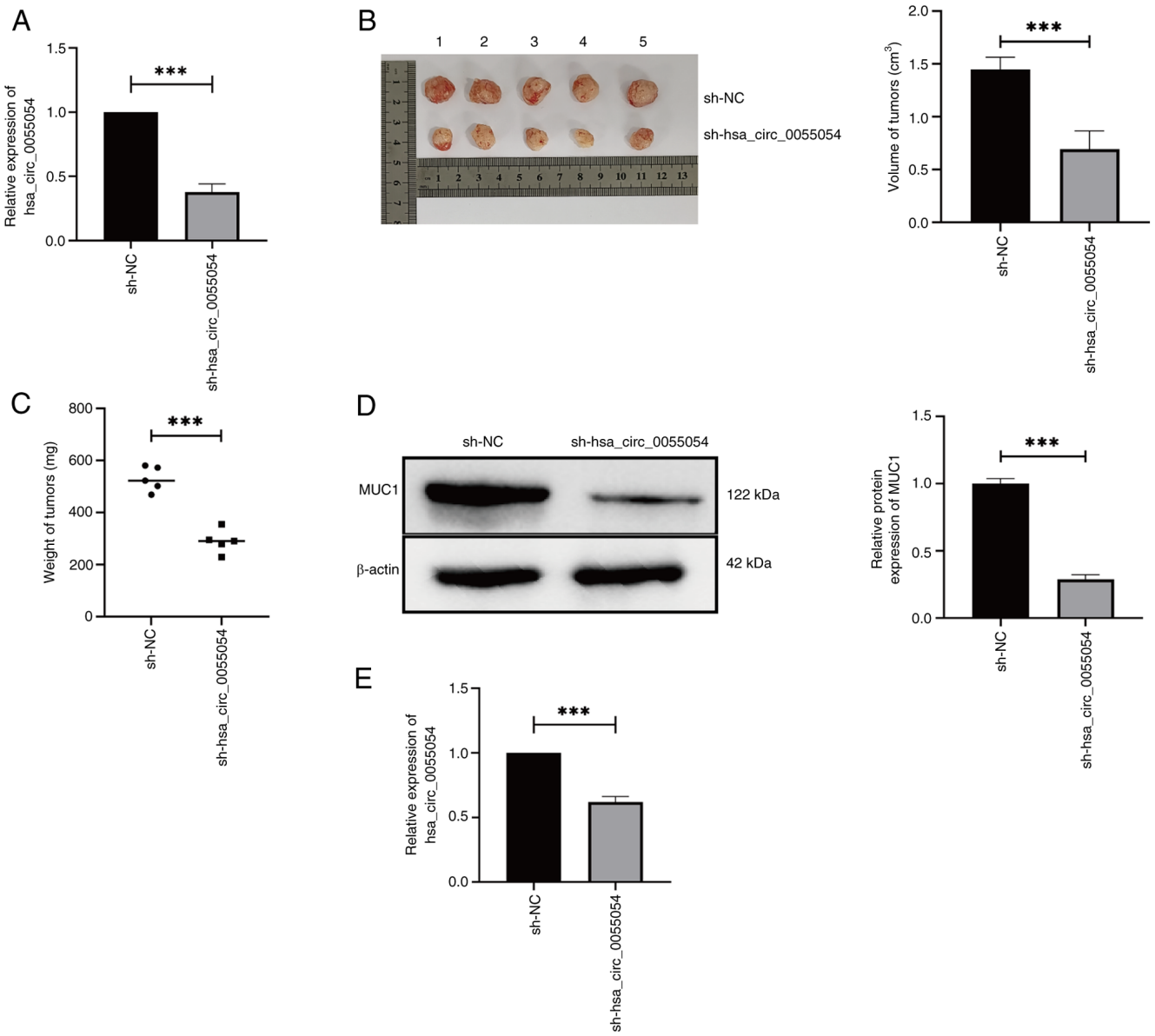

Figure 7. hsa_circ_0055054 knockdown inhibits HCC growth *in vivo*. (A) hsa_circ_0055054 expression in MHCC97L cells following transfection with sh-hsa_circ_0055054 compared with sh-NC, assessed using reverse transcription-quantitative PCR. (B) Tumorigenic volume and (C) weight of MHCC97L cells following transfection with sh-hsa_circ_0055054 *in vivo* compared with that of the sh-NC group. (D) Western blotting for the detection of MUC1 expression in subcutaneous tumors formed by MHCC97L cells following transfection with sh-hsa_circ_0055054 compared with sh-NC. (E) hsa_circ_0055054 expression in subcutaneous tumors formed by MHCC97L cells following transfection with sh-hsa_circ_0055054 compared with sh-NC, assessed using reverse transcription-quantitative PCR. ***P<0.001. MUC1, mucin 1; sh, short hairpin RNA; NC, negative control; circ, circular RNA; HCC, hepatocellular carcinoma.

Blank group. Following transfection, cell phenotype experiments were performed, which revealed that transfection with si-hsa_circ_0055054 significantly inhibited the migration (Fig. 6C), invasion (Fig. 6D) and proliferation (Fig. 6E) of MHCC97L cells to varying degrees compared with the Blank group.

To confirm whether hsa_circ_0055054 regulates MUC1 expression by binding to miR-122-5p, subsequent rescue experiments were performed. Si-NC, si-hsa_circ_0055054 co-transfected with miR-122-5p inhibitor-NC, and si-hsa_circ_0055054 co-transfected with miR-122-5p inhibitor were compared with si-hsa_circ_0055054, respectively. The results indicated that the introduction of an miR-122-5p inhibitor could partially restore the decreased expression of MUC1 due to the suppression of hsa_circ_0055054 (Fig. 6F) and that hsa_circ_0055054 promoted MHCC97L cell proliferation, migration and invasion by binding to miR-122-5p.

hsa_circ_0055054 knockdown inhibits HCC growth in vivo. The RT-qPCR results indicated that the expression of hsa_circ_0055054 was significantly lower in the experimental group sh-hsa_circ_0055054 compared with that in the control group sh-NC. These findings confirmed the successful generation of MHCC97L cells stably transfected with sh-hsa_circ_0055054 (Fig. 7A). The results showed that MHCC97L cells transfected with sh-hsa_circ_0055054 formed subcutaneous tumors of significantly lower volume (Fig. 7B) and weight (Fig. 7C) compared with cells transfected with sh-NC. Subsequently, a significant reduction in MUC1 (Fig. 7D) and hsa_circ_0055054 (Fig. 7E) expression were demonstrated

in the subcutaneous tumors formed by MHCC97L cells transfected with sh-hsa_circ_0055054 compared with those transfected with sh-NC. The aforementioned animal experiments provided evidence that hsa_circ_0055054 knockdown successfully inhibited HCC progression.

Discussion

Previous studies have reported that MUC1 overexpression in several tumor settings, such as thyroid cancer (22), clear cell renal cell carcinoma (23) and breast carcinoma (24), promotes tumor progression. With the development of bioinformatics and molecular biology, the mechanism through which MUC1 may promote HCC progression has been studied extensively. MUC1 may diminish the impact of mitochondrial apoptotic factors and shield HCC cells from anticancer genotoxic agents (25). In established tumors, high levels of MUC1 may hinder the proliferation of cytotoxic T lymphocyte (CTL) cells or cause CTL death, thereby weakening the destructive effect of immune cells (26). In addition, Wang *et al* (27) and Bozkaya *et al* (28) identified a cooperative interaction of MUC1 with the JNK/TGF-β or HGF/c-Met signaling pathway during hepatocarcinogenesis. In combination, these findings indicated that MUC1 has potential as a tumor biomarker for biological treatment (29-31). Furthermore, the search for the upstream regulatory mechanisms of MUC1 has become a new area of research interest in the field of tumor therapy (8). The present study demonstrated that MUC1 expression was significantly higher in HCC tissues and cell lines compared with corresponding adjacent normal tissues and normal liver cells. Furthermore, bioinformatics analysis revealed that patients with a high MUC1 expression in HCC had lower survival rates; however, bioinformatics analysis also demonstrated that MUC1 was not significantly associated with the clinical characteristics of patients with HCC. The results that appeared to be contradictory lead to the investigation of the potential ability of MUC1 inhibition in HCC to prevent HCC progression. The present study demonstrated that the inhibition of MUC1 expression in MHCC97L cells suppressed the proliferation, migration and invasion of MHCC97L cells.

Epigenetics, a heritable change in the function of a gene without a change in the DNA sequence of the gene, ultimately leads to a change in phenotype. The regulation of gene transcription by non-coding RNAs through certain mechanisms is one of the forms of epigenetics (32). For example, several diseases are treated by altering the expression of certain circRNAs and miRNAs in the organism in such a way as to affect their downstream targets in different signaling pathways. Several RNA therapies are currently in clinical use (33). Therefore, targeted therapy of non-coding RNA (such as miRNA and circRNA) holds promise for the treatment of several diseases.

miRNA is a post-transcriptional regulatory factor that decreases the expression of target genes by acting on the mRNA transcribed from genes (34). Previous studies have reported that miR-122-5p is an abundant and conserved liver-specific miRNA that regulates liver metabolism and functions as a tumor suppressor (35-38); however, the interpretation of the miR-122-5p target network remains incomplete. The present study demonstrated that miR-122-5p expression was significantly lower in HCC tissues compared with corresponding adjacent normal tissues, which was consistent with the results of Luna *et al* (39). Notably, the bioinformatics results of the current study suggested that miR-122-5p can bind with MUC1 and regulate its expression. MHCC97L cells were transfected with miR-122-5p mimic and miR-122-5p inhibitor, respectively, with the aim of detecting MUC1 protein expression to demonstrate that miR-122-5p negatively regulates MUC1 expression. Furthermore, inhibition of miR-122-5p promoted MUC1 expression in MHCC97L cells, which complemented the subsequent rescue experiments. These findings were confirmed by dual-luciferase reporter assays and cell function experiments, and indicated that the decreased expression of miR-122-5p in MHCC97L cells promotes MUC1 overexpression, which accelerates MHCC97L cell proliferation, migration and invasion.

There is increasing evidence that circRNAs serve a significant regulatory role in disease through interactions with disease-associated miRNAs (40-42). In HCC, circ-GPR173B (14), circ-ZEB1 (15) and circ-cSMARCA5 (16) have been reported to regulate the growth and metastasis of HCC by acting as sponges for different miRNAs. The hsa_circ_0055054 is formed through the cyclization of exons 10-11 of the glucosamine-fructose-6-phosphate aminotransferase isomerizing 1 (GFPT1) gene. Previous studies have reported that GFPT1 may contribute to the progression of cervical (43), pancreatic (44) and esophageal cancer (45), but the function of hsa_circ_0055054 remains unknown. The present study demonstrated that the expression of hsa_circ_0055054 was significantly higher in HCC tissues compared with the corresponding adjacent normal tissues, and that it binds to miR-122-5p. Furthermore, the present study demonstrated that hsa_circ_0055054 knockdown in MHCC97L cells led to a reduction in MUC1 expression and inhibited the proliferation, migration and invasion of MHCC97L cells. Furthermore, rescue experiments revealed that hsa_circ_0055054 inhibited the phenotypic function of HCC cells through a mechanism dependent on MUC1 by upregulating miR-122-5p.

To determine whether hsa_circ_0055054 knockdown could inhibit the proliferation, migration and invasion of MHCC97L cells *in vivo*, animal experiments were performed. Lentiviral packaging was used to construct cells that could stably proliferate for a long period of time in animals using si-hsa_circ_0055054 sequences previously validated in cellular experiments. The results were consistent with aforementioned cellular experiments, suggesting that the hsa_circ_0055054/miR-122-5p/MUC1 regulatory axis may serve a crucial role in HCC progression.

The present study had certain limitations; it investigated whether hsa_circ_0055054 could regulate MUC1 expression through miR-122-5p, but did not investigate its pathway and mechanism of action; meanwhile, other upstream regulatory mechanisms of MUC1 need to be explored. In addition, it is necessary to assess whether hsa_circ_0055054 and miR-122-5p can influence the development of HCC by affecting other miRNAs and mRNAs, and this is a topic that requires further investigation in the future. Finally, since MUC1 can also serve an important role in several tumors, further investigation is required to determine the role of the hsa_circ_0055054/miR-122-5p/MUC1 regulatory axis in other tumors.

In conclusion, the findings of the current study indicate that hsa_circ_0055054 knockdown in MHCC97L cells can lead to the increased expression of miR-122-5p and decreased expression of MUC1. This can result in the inhibition of

proliferation, migration and invasion of HCC cells. Therefore, both hsa_circ_0055054 and miR-122-5p show promise as future targets for the clinical treatment of HCC.

Acknowledgements

Not applicable.

Funding

No funding was received.

Availability of data and materials

The data generated in the present study may be requested from the corresponding author.

Authors' contributions

PH and HZ conceived the project. PH and QL performed the experiments. PH collected the data and drafted the manuscript. HZ made contributions to the conception and design of the study, as well as to the revision and correction of the manuscript. All authors have read and approved the final manuscript . PH, QL and HZ confirm the authenticity of all the raw data.

Ethics approval and consent to participate

The present study was approved by the Ethics Committee of Third Hospital of Shanxi Medical University, Shanxi Bethune Hospital (approval no. YXLL-2023-226) and the Animal Ethics Committee of Shanxi Provincial People's Hospital (approval no. 2023-451).

Patient consent for publication

Not applicable.

Competing interests

The authors declare that they have no competing interests.

References

1. Sung H, Ferlay J, Siegel RL, Laversanne M, Soerjomataram I, Jemal A and Bray F: Global cancer statistics 2020: GLOBOCAN estimates of incidence and mortality worldwide for 36 cancers in 185 countries. CA Cancer J Clin 71 209-249, 2021.
2. Farazi PA and DePinho RA: Hepatocellular carcinoma pathogenesis: From genes to environment. Nat Rev Cancer 6: 674-687, 2006.
3. Junttila MR and de Sauvage FJ: Influence of tumour microenvironment heterogeneity on therapeutic response. Nature 501: 346-354, 2013.
4. Quail DF and Joyce JA: Microenvironmental regulation of tumor progression and metastasis. Nat Med 19: 1423-1437, 2013.
5. Ringel J and Löhr M: The MUC gene family: Their role in diagnosis and early detection of pancreatic cancer. Mol Cancer 2: 9, 2003.
6. Bhatia R, Gautam SK, Cannon A, Thompson C, Hall BR, Aithal A, Banerjee K, Jain M, Solheim JC, Kumar S and Batra SK: Cancer-associated mucins: Role in immune modulation and metastasis. Cancer Metastasis Rev 38: 223-236, 2019.
7. Li W, Han Y, Sun C, Li X, Zheng J, Che J, Yao X and Kufe D: Novel insights into the roles and therapeutic implications of MUC1 oncoprotein via regulating proteins and non-coding RNAs in cancer. Theranostics 12: 999-1011, 2022.
8. Nabavinia MS, Gholoobi A, Charbgoo F, Nabavinia M, Ramezani M and Abnous K: Anti-MUC1 aptamer: A potential opportunity for cancer treatment. Med Res Rev 37: 1518-1539, 2017.
9. Ren J, Agata N, Chen D, Li Y, Yu WH, Huang L, Raina D, Chen W, Kharbanda S and Kufe D: Human MUC1 carcinoma-associated protein confers resistance to genotoxic anticancer agents. Cancer Cell 5: 163-175, 2004.
10. Nath S and Mukherjee P: MUC1: A multifaceted oncoprotein with a key role in cancer progression. Trends Mol Med 20: 332-342, 2014.
11. Ye J, Wei X, Shang Y, Pan Q, Yang M, Tian Y, He Y, Peng Z, Chen L, Chen W and Wang R: Core 3 mucin-type O-glycan restoration in colorectal cancer cells promotes MUC1/p53/miR-200c-dependent epithelial identity. Oncogene 36: 6391-6407, 2017.
12. Roy LD, Sahraei M, Subramani DB, Besmer D, Nath S, Tinder TL, Bajaj E, Shanmugam K, Lee YY, Hwang SI, *et al*: MUC1 enhances invasiveness of pancreatic cancer cells by inducing epithelial to mesenchymal transition. Oncogene 30: 1449-1459, 2011.
13. Yuan SF, Li KZ, Wang L, Dou KF, Yan Z, Han W and Zhang YQ: Expression of MUC1 and its significance in hepatocellular and cholangiocarcinoma tissue. World J Gastroenterol 11: 4661-4666, 2005.
14. Liu L, Gu M, Ma J, Wang Y, Li M, Wang H, Yin X and Li X: CircGPR137B/miR-4739/FTO feedback loop suppresses tumorigenesis and metastasis of hepatocellular carcinoma. Mol Cancer 21: 149, 2022.
15. Liu W, Zheng L, Zhang R, Hou P, Wang J, Wu L and Li J: Circ-ZEB1 promotes PIK3CA expression by silencing miR-199a-3p and affects the proliferation and apoptosis of hepatocellular carcinoma. Mol Cancer 21: 72, 2022.
16. Yu J, Xu QG, Wang ZG, Yang Y, Zhang L, Ma JZ, Sun SH, Yang F and Zhou WP: Circular RNA cSMARCA5 inhibits growth and metastasis in hepatocellular carcinoma. J Hepatol 68: 1214-1227, 2018.
17. Zhou WY, Cai ZR, Liu J, Wang DS, Ju HQ and Xu RH: Circular RNA: Metabolism, functions and interactions with proteins. Mol Cancer 19: 172, 2020.
18. Ni J, Bucci J, Chang L, Malouf D, Graham P and Li Y: Targeting MicroRNAs in prostate cancer radiotherapy. Theranostics 7: 3243-3259, 2017.
19. Han B, Chao J and Yao H: Circular RNA and its mechanisms in disease: From the bench to the clinic. Pharmacol Ther 187: 31-44, 2018.
20. Kristensen LS, Jakobsen T, Hager H and Kjems J: The emerging roles of circRNAs in cancer and oncology. Nat Rev Clin Oncol 19: 188-206, 2022.
21. Livak KJ and Schmittgen TD: Analysis of relative gene expression data using real-time quantitative PCR and the 2(-Delta Delta C(T)) method. Methods 25: 402-408, 2001.
22. Patel KN, Maghami E, Wreesmann VB, Shaha AR, Shah JP, Ghossein R and Singh B: MUC1 plays a role in tumor maintenance in aggressive thyroid carcinomas. Surgery 138: 994-1002, 2005.
23. Lucarelli G, Netti GS, Rutigliano M, Lasorsa F, Loizzo D, Milella M, Schirinzi A, Fontana A, Di Serio F, Tamma R, *et al*: MUC1 expression affects the immunoflogosis in renal cell carcinoma microenvironment through complement system activation and immune infiltrate modulation. Int J Mol Sci 24: 4814, 2023.
24. Schroeder JA, Adriance MC, Thompson MC, Camenisch TD and Gendler SJ: MUC1 alters beta-catenin-dependent tumor formation and promotes cellular invasion. Oncogene 22: 1324-1332, 2003.
25. Yuan H, Wang J, Wang F, Zhang N, Li Q, Xie F, Chen T, Zhai R, Wang F, Guo Y, *et al*: Mucin 1 gene silencing inhibits the growth of SMMC-7721 human hepatoma cells through Bax-mediated mitochondrial and caspase-8-mediated death receptor apoptotic pathways. Mol Med Rep 12: 6782-6788, 2015.
26. Bose M and Mukherjee P: Microbe-MUC1 crosstalk in cancer-associated infections. Trends Mol Med 26: 324-336, 2020.
27. Wang J, Ni WH, Hu KB, Zhai XY, Xie F, Jie J, Zhang NN, Jiang LN, Yuan HY and Tai GX: Targeting MUC1 and JNK by RNA interference and inhibitor inhibit the development of hepatocellular carcinoma. Cancer Sci 108: 504-511, 2017.
28. Bozkaya G, Korhan P, Cokaklı M, Erdal E, Sağol O, Karademir S, Korch C and Atabey N: Cooperative interaction of MUC1 with the HGF/c-Met pathway during hepatocarcinogenesis. Mol Cancer 11: 64, 2012.
29. Apostolopoulos V, Stojanovska L and Gargosky SE: MUC1 (CD227): A multi-tasked molecule. Cell Mol Life Sci 72: 4475-4500, 2015.

30. Carson DD: The cytoplasmic tail of MUC1: A very busy place. Sci Signal 1: pe35, 2008.
31. Supruniuk K and Radziejewska I: MUC1 is an oncoprotein with a significant role in apoptosis (review). Int J Oncol 59: 68, 2021.
32. Villanueva L, Álvarez-Errico D and Esteller M: The contribution of epigenetics to cancer immunotherapy. Trends Immunol 41: 676-691, 2020.
33. Winkle M, El-Daly SM, Fabbri M and Calin GA: Noncoding RNA therapeutics-challenges and potential solutions. Nat Rev Drug Discov 20: 629-651, 2021.
34. Wang N, Zheng J, Chen Z, Liu Y, Dura B, Kwak M, Xavier-Ferrucio J, Lu YC, Zhang M, Roden C, *et al*: Single-cell microRNA-mRNA co-sequencing reveals non-genetic heterogeneity and mechanisms of microRNA regulation. Nat Commun 10: 95, 2019.
35. Wang L, Zhang Z and Wang FS: The efficacy of miRNA122, a novel therapeutic target, for predicting the progression of hepatocellular carcinoma (HCC). Cell Mol Immunol 9: 103-104, 2012.
36. Bandiera S, Pfeffer S, Baumert TF and Zeisel MB: miR-122-a key factor and therapeutic target in liver disease. J Hepatol 62: 448-457, 2015.
37. Nakao K, Miyaaki H and Ichikawa T: Antitumor function of microRNA-122 against hepatocellular carcinoma. J Gastroenterol 49: 589-593, 2014.
38. Xu Y, Xia F, Ma L, Shan J, Shen J, Yang Z, Liu J, Cui Y, Bian X, Bie P and Qian C: MicroRNA-122 sensitizes HCC cancer cells to adriamycin and vincristine through modulating expression of MDR and inducing cell cycle arrest. Cancer Lett 310: 160-169, 2011.
39. Luna JM, Barajas JM, Teng KY, Sun HL, Moore MJ, Rice CM, Darnell RB and Ghoshal K: Argonaute CLIP defines a deregulated miR-122-bound transcriptome that correlates with patient survival in human liver cancer. Mol Cell 67: 400-410. e7, 2017.
40. Chen S, Zhang Y, Ding X and Li W: Identification of lncRNA/circRNA-miRNA-mRNA ceRNA network as biomarkers for hepatocellular carcinoma. Front Genet 13: 838869, 2022.
41. Singh D, Kesharwani P, Alhakamy NA and Siddique HR: Accentuating CircRNA-miRNA-transcription factors axis: A conundrum in cancer research. Front Pharmacol 12: 784801, 2022.
42. Xiong DD, Dang YW, Lin P, Wen DY, He RQ, Luo DZ, Feng ZB and Chen G: A circRNA-miRNA-mRNA network identification for exploring underlying pathogenesis and therapy strategy of hepatocellular carcinoma. J Transl Med 16: 220, 2018.
43. Li D, Guan M, Cao X, Zha ZQ, Zhang P, Xiang H, Zhou Y, Peng Q, Xu Z, Lu L and Liu G: GFPT1 promotes the proliferation of cervical cancer via regulating the ubiquitination and degradation of PTEN. Carcinogenesis 43: 969-979, 2022.
44. Gong Y, Qian Y, Luo G, Liu Y, Wang R, Deng S, Cheng H, Jin K, Ni Q, Yu X, *et al*: High GFPT1 expression predicts unfavorable outcomes in patients with resectable pancreatic ductal adenocarcinoma. World J Surg Oncol 19: 35, 2021.
45. Zhang C, Lian H, Xie L, Yin N and Cui Y: LncRNA ELFN1-AS1 promotes esophageal cancer progression by up-regulating GFPT1 via sponging miR-183-3p. Biol Chem 401: 1053-1061, 2020.